# CORROSION BEHAVIORS OF THE IRON-BASED AND Ni-BASED BRAZING FILLER METALS BRAZED ON THE STAINLESS STEELS IN A SOLUTION OF 3.5MASS% NaCl

*Satoshi Sunada[1)]*, Masahiko Hataheyama[1)], Haruna Motoya[2)], Norio Nunomura[3)]*
*[1)] University of Toyama, Graduate School of Science and Engineering for Research, Toyama Japan*
*[2)] University of Toyama, Undergraduate Student, [Current Address TSUNE SEIKI CO., LTD, Toyama Japan*
*[3)] University of Toyama, Information Technology Center, Toyama Japan*

Received: 11.08.2017
Accepted: 29.09.2017

**Corresponding author: e-mail: suna@eng.u-toyama.ac.jp, Tel.: +81-76-445-6818, Graduate School of Science and Engineering for Research, University of Toyama, 3190 Gofuku, Toyama 930-8555, Japan*

**Abstract**
The corrosion resistance was studied electrochemically for an iron-based brazing filler metal F300 and a Ni-based brazing filler metal Ni613. Both austenitic stainless steel SUS316 and ferritic stainless steel SUS444 were used as base metals for these brazing filling metals. F300 showed a higher corrosion rate than those of Ni613 and both base metals and was less corrosion-resistive. While Ni613 showed a stronger depression effect of an anodic reaction than those of base metals, F300 showed little depression effect of the reaction. As an Fe-Ni phase dissolved preferentially in F300 and a finite laminated corrosive morphology was observed, the corrosion progression along a depth direction was suggested. These corrosion behaviors depend on the difference of chemical composition of these brazing filler metals.

**Keywords:** corrosion rate, passivating film, polarization curve, stainless steel

## 1 Introduction

One of the brazing filler metals suitable for high temperature brazing would be a nickel-based brazing filler metal. A Ni-based brazing filling metal is composed of Ni or Ni-Cr alloy and silicon or phosphorous are added for lowering the melting temperature or improvement of its fluidity. Because of its excellent high-temperature strength and high corrosion or oxidation resistance of a brazed connection [1], it has been used in the production processes for EGR coolers, oil coolers or heat exchangers. However, as a majority of its components is Ni, potentially higher production cost due to price fluctuations of a raw material is problematic [2]. Thus, developments of new iron-based brazing filling metals with lesser Ni content are in progress aiming to substitute for existing Ni-based brazing filling metals. A Fe-based brazing filling metal is thought to have the same characteristics as a Ni-based one and excellence in strength or corrosion resistance is expected. However, specific characteristics have not been revealed yet. In this study, polarization curves were measured for a Ni-base brazing filling metal and Fe-based one when they were brazed to an austenitic stainless steel SUS316 or a ferritic stainless steel SUS444. These stainless steels are mainly used as base metals for current stainless steel products assembled using the brazing process. The corrosion behaviors of brazing filling

DOI 10.12776/ams.v24i1.1025 p-ISSN 1335-1532
e-ISSN 1338-1156

metals were evaluated electrochemically and those of base metals were also evaluated and compared them. Further, corrosion morphology was also evaluated by surficial and cross-sectional SEM images before and after the test.

## 2 Experiment

### 2.1 Specimens and test solution

**Table 1** shows the treatment condition for each sample. Sample A was prepared by placing a predetermined commercially available Ni-based brazing filling metal on a surface of a SUS316 stainless steel and brazed at 1373K for 10 min. in an Ar atmosphere. Sample D was obtained similarly but using a SUS444 stainless steel plate. Samples B and E were also prepared similarly but using Fe-based brazing filling metals for a SUS316 and the SUS444 respectively. Brazed metals of the SUS316 and SUS444 were eliminated by grinding to investigate corrosion behaviors of base metals and were named as sample C and sample F respectively. **Table 2** shows compositions of brazing filling metals and **Table 3** shows compositions of stainless steels. As a pretreatment, ultrasound cleaning was applied for the sample in an acetone fluid for 300s. After being dried up, the sample was fixed to a brass pole and used as a working electrode after applying an insulation coating except for an exposed area of $1.0\times10^{-4}m^2$. A solution of 3.5mass% NaCl (pH=5.4) was used as a test solution.

**Table 1** Treatment condition for each sample

| Sample | Steel grade | Brazing filler metal | Temperature (K) | Processing time (min) | Atmosphere gas |
|---|---|---|---|---|---|
| **A** | SUS316 | Ni613 | 1373 | 10 | Ar |
| **B** | | F300 | | | |
| **C** | | - | | | |
| **D** | SUS444 | Ni613 | | | |
| **E** | | F300 | | | |
| **F** | | - | | | |

**Table 2** The chemical compositions of the base metals

| brazing filler metal | Chemical composition (%) | | | | | | |
|---|---|---|---|---|---|---|---|
| | Ni | Cr | Fe | Si | P | Mn | Cu |
| Ni613 | Bal | 29 | - | 4 | 6 | - | - |
| F300 | 20 | 24 | Bal | 5 | 7 | 5 | 10 |

**Table 3** The chemical compositions of the brazing filler metals

| steel grade | Chemical composition(%) | | | | | | | | | | |
|---|---|---|---|---|---|---|---|---|---|---|---|
| | Cr | Ni | Fe | S | P | Mn | Mo | Si | C | N | Ti,Nb,Zr |
| SUS316 | 16~18 | 10~14 | Bal | ≦0.03 | ≦0.045 | ≦2 | 2~3 | ≦1 | ≦0.08 | - | - |
| SUS444 | 17~20 | - | Bal | ≦0.03 | ≦0.04 | ≦1 | 1.75~2.5 | ≦1 | ≦0.025 | ≦0.025 | few |

### 2.2 Polarization curve measurement

Polarization curves were measured for the samples to investigate corrosion behaviors. A schematic diagram of an instrument used for the measurement is shown in **Fig. 1**. Specimen with

DOI 10.12776/ams.v24i1.1025 p-ISSN 1335-1532
e-ISSN 1338-1156

a reaction area of $1.0\times10^{-4}m^2$ was used as a working electrode and a Pt electrode was used as a counter electrode in a constant temperature bath kept at 298K. An Ag/AgCl(3.33kmol/$m^3$KCl) plate was used as a reference electrode. Interfacial potential of the sample was measured by a capillary attached to an apex of the bridge and referred to a double-junction reference electrode. Potential was regulated by a computer.

Test solution was filled into an H-type cell and degassed with $N_2$ for 1.8ks before the experiment to suppress experimental errors due to dissolved oxygen. A specimen was placed and a cathodic treatment was applied for 300s and a 1.8ks natural immersion was followed for stabilization of the specimen surface, then a polarization curve was measured by sweeping the potential from -0.60V to 1.40V at a sweeping rate of 0.50m/V. Variation of potential with logarithmic current density was plotted as a polarization curve. During the measurement, $N_2$ gas was aerated over a surface of the solution to prevent dissolution of oxygen.

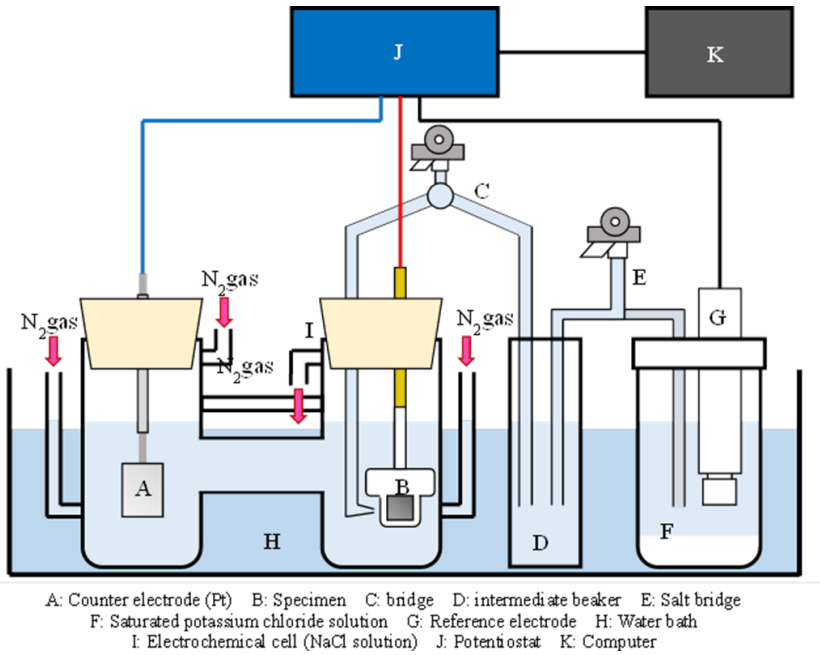


**Fig. 1** Schematic diagram of apparatus for the polarization curve measurement

### 2.3 Specimen surface and cross-sectional observation

The surface and cross-section of each sample were observed using both an optical microscope and a SEM (Hitachi TM3030) before and after the polarization curve measurement to evaluate corrosion morphologies.

### 2.4 Elemental mapping by EPMA

SEM observations for brazing metals confirmed co-existence of dark phases and light phases with different contrasts. An elemental mapping was performed using an EPMA (JEOL, JXA-8230) to analyze constitution of each phase and to determine which phase dissolved preferentially after the polarization curve measurement. Main or common elements contained in the brazing materials were given priority for evaluation.

DOI 10.12776/ams.v24i1.1025 p-ISSN 1335-1532
e-ISSN 1338-1156

## 3 Results and discussion

### 3.1 Polarization curve measurement

**Fig. 2** shows polarization curves obtained in a solution of 3.5mass% NaCl for samples A, B and C. **Table 4** shows corrosion potential $E_{corr}$ and corrosion rate $I_{corr}$ obtained by the Tafel extrapolation method. Comparison of traces of polarization curves revealed that there are clear differences among them in an anodic range in contrast to those in a cathodic range where little difference is shown. Pitting potential $E_{pit}$ of 0.54V was confirmed in sample C composed of a base meatal of SUS316. Fluctuation of the current density is minor from near 0V to just before the pitting potential, indicating suppression of an anodic reaction whereas an abrupt increase in the current density is shown at around the pitting potential. Definitive pitting potential could not be confirmed in the sample A and unlike in the sample C, it does not show an abrupt increase in the current density. In sample B, current density increases rapidly from the corrosion potential, showing no suppression of an anodic reaction. Relationship between the corrosion rate and the corrosion potential can be explained using the Evans diagram shown in **Fig. 6**. A cathodic reaction is represented by a downward line and an anodic reaction is represented by an upward line. Polarization measurements showed that each polarization curve behaves differently in an anodic range. Considering the base metal as a standard, an increase in the corrosion potential and a decrease in the corrosion rate make a slope of the line steeper and a rapid increase in the current density is suppressed, causing suppression of an anodic reaction. When the corrosion potential decreases and the corrosion rate increases, a slope becomes smaller and an anodic reaction is enhanced. Based on these relationships, it can be said that sample A with Ni613

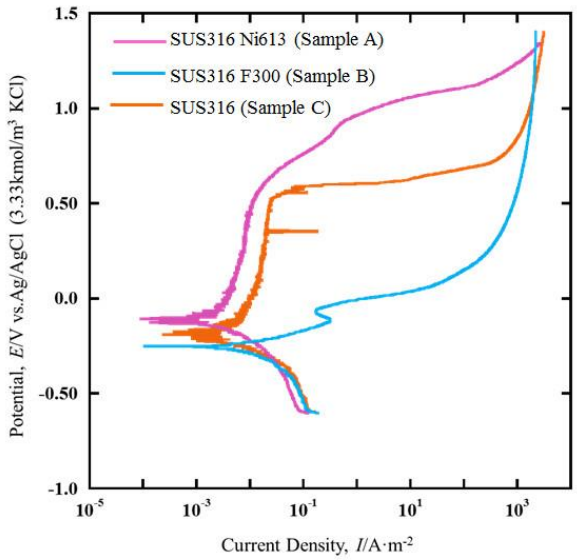


**Fig. 2** Polarization curves of sample A, sample B and sample C measured in 3.5%NaCl solution at 298K

brazed to the SUS316 is the most corrosion-resistive and sample B with F300 brazed to the SUS316 is poorer in corrosion resistance. **Fig. 3** shows corrosion rate plots obtained by the Tafel extrapolation method for comparison. Comparing corrosion rates among these 3 samples, sample B with F300 brazed to a base metal has the highest corrosion rate of $1.0\times10^{-2}$A/m$^2$, and

DOI 10.12776/ams.v24i1.1025 p-ISSN 1335-1532
e-ISSN 1338-1156

sample A with Ni613 brazed to a base metal has the lowest corrosion rate of $1.58\times10^{-3}$A/m$^2$. Comparing these results to that of the base metal sample C without brazing filler metal, the corrosion rate of sample A is 0.75 times higher than that of sample C, showing favorable corrosion resistance, whereas sample B has 4.7 times higher corrosion rate than sample C demonstrating poorer corrosion resistance. Comparing samples A with sample B, corrosion rate of the latter is 6.3 times higher than that of the former, indicating that a Fe-based brazing filling metal F300 cannot accomplish an equivalent corrosion resistance to a Ni-based brazing filling metal Ni613.

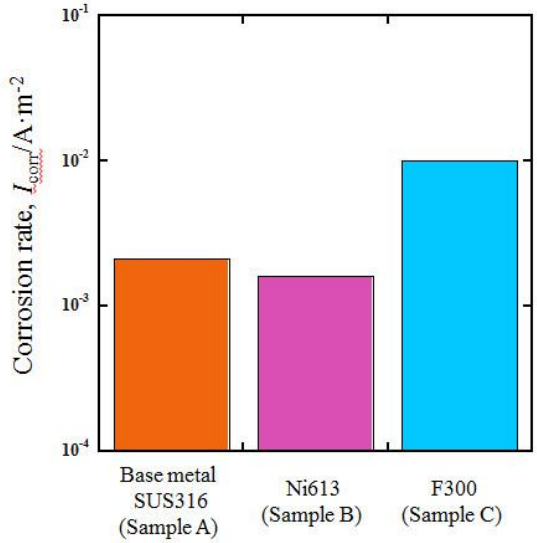


**Fig. 3** Corrosion rate of sample A, sample B and sample C

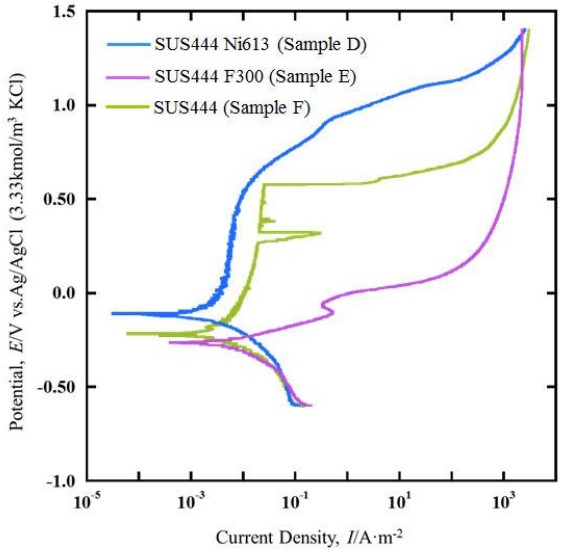


**Fig. 4** Polarization curves of sample D, sample E and sample F measured in 3.5mass%NaCl solution at 298K

DOI 10.12776/ams.v24i1.1025 p-ISSN 1335-1532
e-ISSN 1338-1156

**Fig. 4** shows polarization curves of the sample D, E and F measured in a solution of 3.5%mass% NaCl. **Table 5** shows corrosion potentials and corrosion rates obtained by the Tafel extrapolation method. Comparison of the corrosion rate is shown graphically in **Fig. 6**. Comparing the corrosion rates among these 3 samples, sample D has the highest corrosion rate of $8.41\times10^{-3}$ and sample C has the lowest one of $1.78\times10^{-3}$. Comparing traces of the polarization curve in **Fig. 2** with those in **Fig. 4**, a similarity can be seen between sample A and D and so too with the similarity between sample B and C, and sample C and F. These show that traces of the polarization curve are similar irrespective of the base metal when the same brazing filling metal is given and suggest that a base metal makes little influence on corrosion progression. Followings are also found: base metals SUS316 and SUS444 have similar corrosion resistances; samples A and D that were brazed with the Ni-based brazing filling metal have superior corrosion resistance than samples C and F that were the base metals of them; samples B and E that were brazed with the Fe-based brazing metal have poorer corrosion resistance than samples B and E that were the base metals of them.

**Table 4** Corrosion rate and potential of each brazing filler metal on the SUS316 base metal.

| | Sample A | Sample B | Sample C |
|---|---|---|---|
| Corrosion rate ($A/m^2$) | $1.58\times10^{-3}$ | $1.0\times10^{-2}$ | $2.11\times10^{-3}$ |
| Corrosion potential (V) | -0.11 | -0.25 | -0.19 |

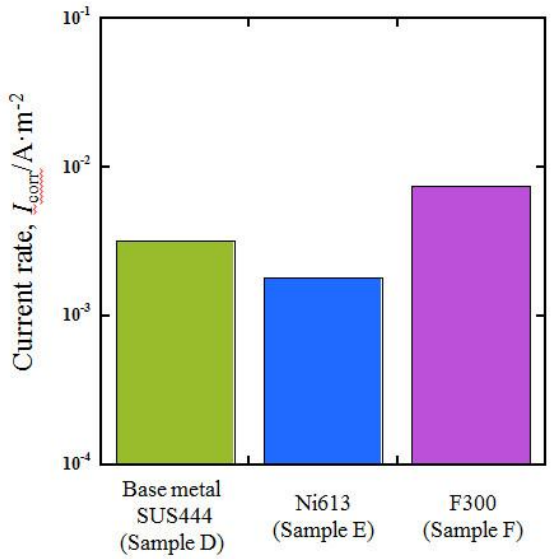


**Fig. 5** Corrosion rates of sample D, sample E and sample F

**Table 5** Corrosion rate and potential of each brazing filler metal on the SUS444 base metal.

| | Sample A | Sample B | Sample C |
|---|---|---|---|
| Corrosion rate ($A/m^2$) | $1.58\times10^{-3}$ | $1.0\times10^{-2}$ | $2.11\times10^{-3}$ |
| Corrosion potential (V) | -0.11 | -0.25 | -0.19 |

DOI 10.12776/ams.v24i1.1025 p-ISSN 1335-1532
e-ISSN 1338-1156

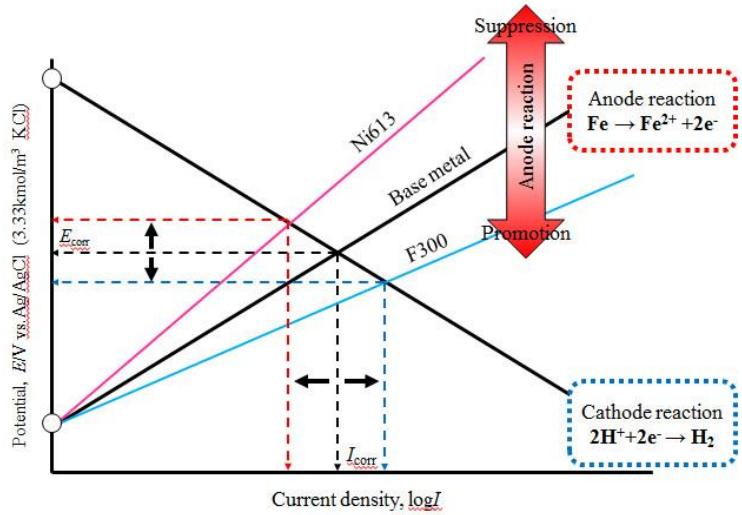


**Fig. 6** Evans diagram

### 3.2 Specimen surface and cross-sectional observation

Surface and cress-sectional morphologies of each sample were observed before and after the measurement of the polarization curve. **Fig. 7** shows optical-microscopic images of samples C and F obtained after the measurement of polarization curve. Pits were observed on the surface of each sample. This can be attributed to corrosion progression due to partial breakdown of a passivating film on a surface of the stainless steel attacked by chloride ions in a solution.

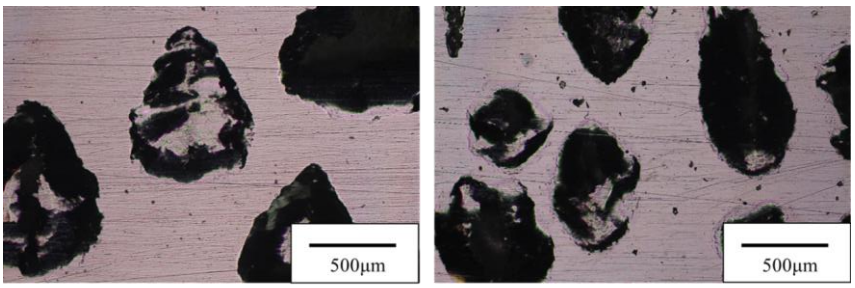


(a) SUS316 (sampleC) (b) SUS444 (sampleF)

**Fig. 7** Optical microphotographs of the surface of sample C and sample F after polarization curve measurement

Surface and cross-sectional SEM images of sample A before and after the measurement of polarization curve are shown in **Fig. 8**. **Fig. 8** (a) shows co-existence of two phases with different contrast, one is a lighter phase and another is a darker phase. Although the formation of corrosion seemed uniform throughout a specimen surface to the an-aided eye, **Fig. 8** (b) shows that there exists preferentially dissolved regions after the polarization curve measurement. It can be assumed that one of the two phases of the brazing filling metal dissolved preferentially into the matrix to induce this form of corrosion. **Fig. 8** (b) also shows small regions corroded to the depth direction. Similar morphology was also observed in sample D (**Fig. 10**).

DOI 10.12776/ams.v24i1.1025 p-ISSN 1335-1532
e-ISSN 1338-1156

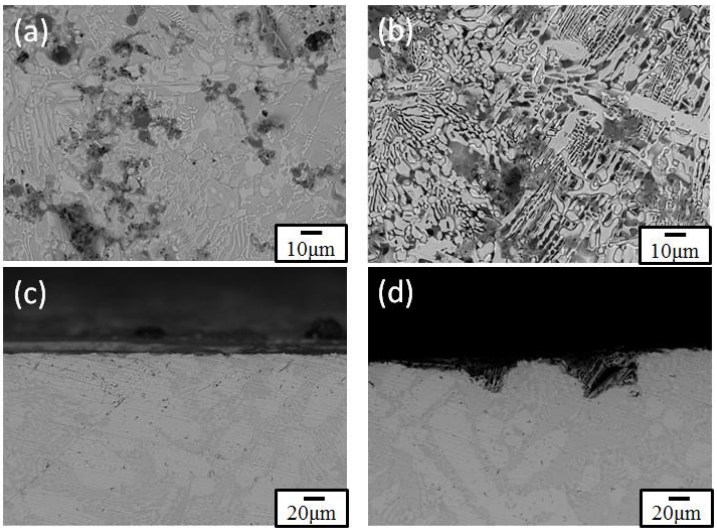


**Fig. 8** SEM micrographs of the sample A surface before and after polarization curve measurement. (a) and (c) are before measurements. (c) and (d) shows cross-section of the samples

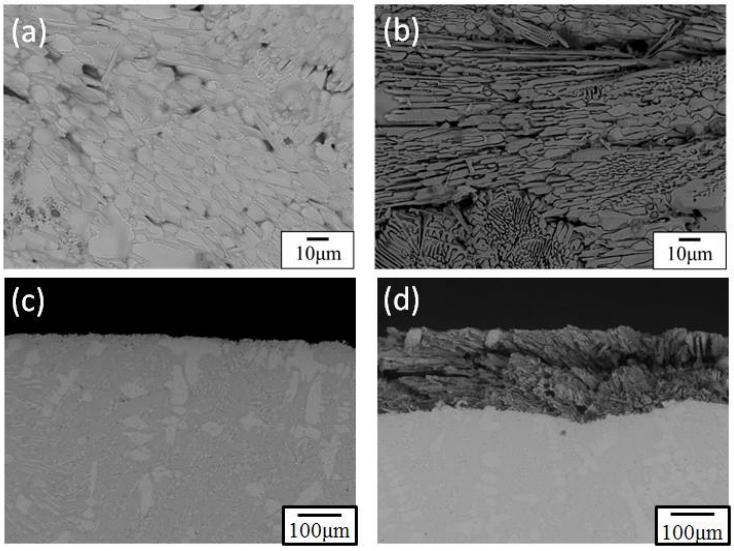


**Fig. 9** SEM micrographs of the sample B surface before and after polarization curve measurement. (a) and (c) are before measurements. (c) and (d) shows cross-section of the samples

SEM images of the specimen surface and the cross-section in sample B before and after the polarization curve measurement are shown in **Figs. 9**. **Fig. 9** (b) shows the similar corrosion morphology of sample B to sample A with preferentially dissolved regions. **Fig. 9** (d) shows that a whole measuring surface is corroded around 200μm in depth and dissolution to form a finite

DOI 10.12776/ams.v24i1.1025 p-ISSN 1335-1532
e-ISSN 1338-1156

layered texture can be observed. Phase separation into two parts with different contrasts was also seen in F300, indicating preferential dissolution of either one of the two phases to form morphology similar to that seen in **Figs. 9** (b) and (d). Similar corrosion form was also confirmed in sample E (**Fig. 11**).

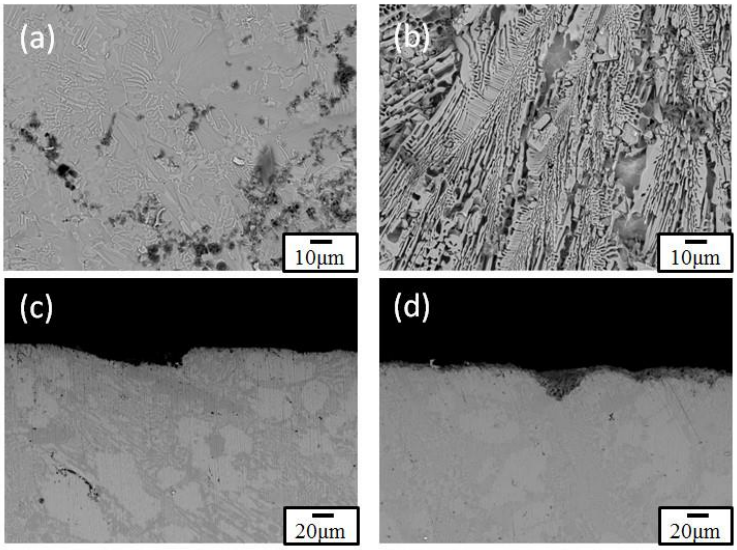


**Fig. 10** SEM micrographs of the sample D surface before and after polarization curve measurement. (a) and (c) are before measurements. (c) and (d) shows cross-section of the samples

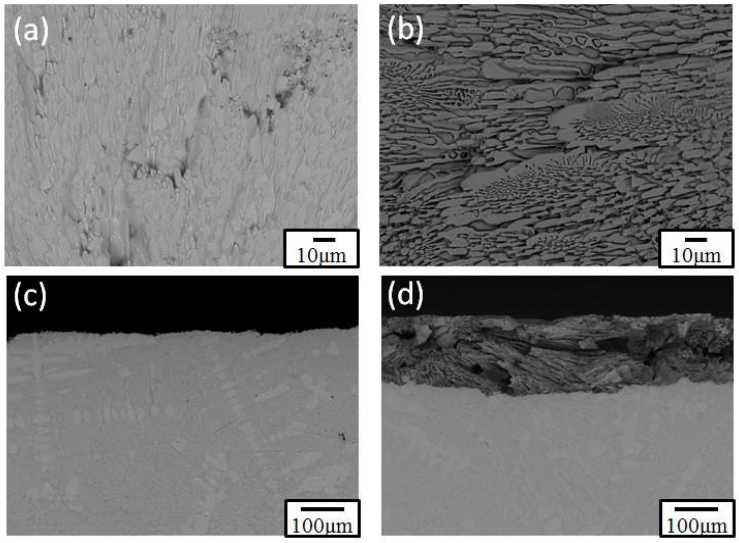


**Fig. 11** SEM micrographs of the sample E surface before and after polarization curve measurement. (a) and (c) are before measurements. (c) and (d) shows cross-section of the samples

DOI 10.12776/ams.v24i1.1025 p-ISSN 1335-1532
e-ISSN 1338-1156

Samples A, D, B and E were compared after polarization curve measurements. Samples A and D were Ni361 brazed samples while B and E were F300 brazed samples and the base metals were two kind of stainless steels. F300 brazed samples had been deteriorated more heavily than Ni316 brazed samples. As F300 contains Fe, it can be assumed that chloride ions contained in a NaCl solution affected heavily. On the other hand, corrosion progression in the depth direction was rarely seen in Ni613 brazed samples although a preferentially dissolved phase was confirmed. Nor pits seen in each base metal were not observed, indicating superior pitting corrosion resistance. Thus, it can be said that a Ni613 is more corrosion resistive than a F300 in a NaCl solution.

### 3.3 Elemental mapping using EPMA

**Fig. 12** shows elemental mappings of a cross-section of sample A obtained using an EPMA, revealing distributions of Ni, Cr, P and Si contained in the Ni613. Comparing them with a SEM image in **Fig.12** (a), it can be seen that a phase (α) in the SEM image corresponds to a Ni rich region where Cr content is low and P is scarcely concentrated. A phase (β) corresponds to a Cr and P concentrated region. **Fig. 13** shows EPMA elemental mappings of a cross-section of a sample B and demonstrates distributions of Fe, Ni, Cr, P and Si contained in the F300. Comparing them with a SEM image in **Fig. 9** (d), it can be seen that a phase (α) in a SEM image corresponds to a Fe and Ni rich region where Cr content is low and contains little P as in the case of the Ni613. A phase (β) shows concentrated Cr and P. Corrosion progression of 200μm in depth seen in **Fig. 11** is considered to be caused by preferential dissolution of the phase (α) in F300 which contains easily ionizable Fe in plenty and is affected strongly by a corrosive solution to form a corrosive morphology seen in **Fig. 9** (b) and (d).

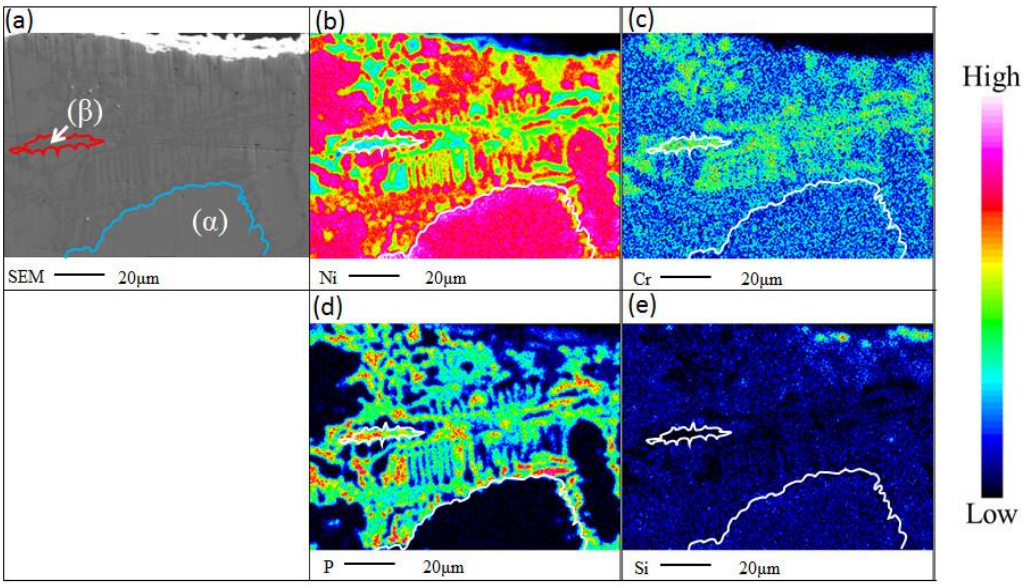


**Fig. 12** Elemental mappings of a cross-section of sample A obtained using an EPMA, revealing distributions of (b)Ni, (c) Cr, (d)P and (e)Si contained in the Ni613

DOI 10.12776/ams.v24i1.1025 p-ISSN 1335-1532
e-ISSN 1338-1156

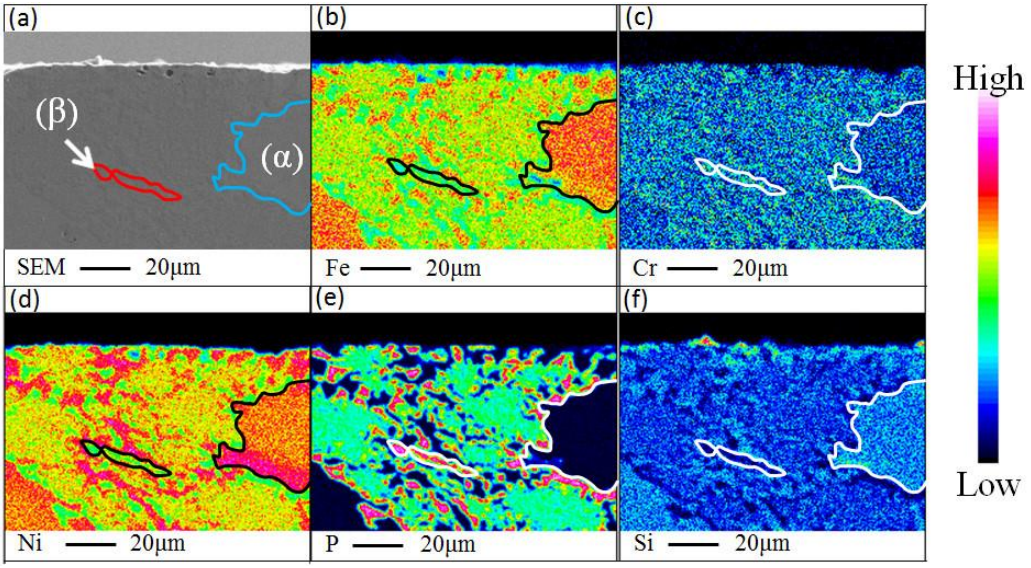


**Fig. 13** Elemental mappings of a cross-section of sample B obtained using an EPMA, revealing distributions of (b)Fe, (c) Cr, (d) Ni, (d) P and (e) Si contained in the F300

## 4 Conclusions

Corrosion characteristics of a Ni-base brazing filling metal Ni613 and a Fe-base brazing filling metal F300 were studied by using an austenitic stainless steel SUS316 and a ferritic stainless steel F300 as base metals and the following conclusions were drawn.

1) The polarization curve showed that Ni623 is adequately corrosion-resistive as a corrosion rate of Ni613 was small enough compared to those of base metals. By contrast, a corrosion rate of F300 was higher than those of base metals and Ni316, showing inadequate corrosion resistance of F300. Pitting potential could be confirmed in both base metals, i.e. SUS316 and SUS444.
2) Difference in the corrosion behavior among samples was appeared in an anodic region. Ni613 showed stronger suppression of an anodic reaction than both base metals showed, while F300 gave little indication of the suppression of an anodic reaction.
3) SEM observation demonstrated the occurrence of pitting corrosions in both base metals after polarization potential measurements. Ni316 showed a slight corrosion progression in depth direction in a partial surface area. Whole surface of F300 observed was corroded and corrosion progression around 200μm in depth was observed. They might be affected strongly in a corrosive NaCl solution.
4) According to the results of elemental analysis using an EPMA, a light phase seen in a SEM image of N613 corresponded to a Ni rich region where a minute content of Cr was detected and P was not concentrated. A dark phase seen in a SEM image corresponded to a Cr and P rich region. In the case of F300, a light one corresponded to a Fe and Ni rich region and dark one corresponded to a Cr and P rich region. It is considered that a Fe-Ni phase in F300 dissolved preferentially to form a finite layered corrosive morphology and corrosion progression in the depth direction was suggested.

DOI 10.12776/ams.v24i1.1025 p-ISSN 1335-1532
e-ISSN 1338-1156

**References**

[1] T. Onzawa, T. Matsu: *The first step in brazing (The series of welding vol. 2)*, Sanpo Publication Incorporated, 2013, ISBN-13: 9784883182329, (written in Japanese)

[2] U. Persson: *Iron-based brazing filler metals for high temperature brazing of stainless steel*, Medical Wire & Components, 2015, p. 38-41

DOI 10.12776/ams.v24i1.1025 p-ISSN 1335-1532
e-ISSN 1338-1156